Technische Universität Darmstadt | Merckstraße 25 | 64283 Darmstadt

Projektträger DESY
Deutsches Elektronen-Synchrotron DESY
Notkestr. 85
22607 Hamburg

BMBF-Forschungsvorhaben
Thema: "R&D BESCHLEUNIGER: Neuartiger DC-Strahlstrom-Transformator" Förderkennzeichen 05P12RDRBG
Verwendungsnachweis 2015 – fachlicher Schlussbericht

30. November 2015

Sehr geehrte Damen und Herren,

in der Anlage übersende ich Ihnen den Verwendungsnachweis 2015 / fachlichen Schlussbericht des o.g. Projekts.

Ich darf mich nochmals sehr herzlich für die Möglichkeit bedanken dieses Forschungsvorhaben durchzuführen und stehe Ihnen für Fragen gerne zur Verfügung.

Mit freundlichen Grüßen

Fachbereich 18
Elektrotechnik und Informationstechnik
Institut für Datentechnik
FG Integrierte Elektronische Systeme
Integrated Electronic Systems Lab

Prof. Dr.-Ing. Klaus Hofmann
Merckstraße 25
64283 Darmstadt

Tel.: +49 6151 16 - 5136
Fax: +49 6151 16 - 4936
Klaus.Hofmann@ies.tu-darmstadt.de

Final Technical Report

❖ Introduction

This document is the final technical report for the project "R & D Accelerators: Novel-DC Beam Current Transformer". It highlights the completed tasks during the period from 1st of January to 30th of June 2015. The main objective of the project is to design a Novel DC Current Transformer (N-DCCT) for the synchrotron SIS100. This accelerator will be part of the "Facility for Antiproton and Heavy Ion Research (FAIR)" project. The N-DCCT design presented in this project can be considered as an extension to the primary design of Open-loop N-DCCT device proposed by GSI and University of Kassel in 2008. The design was based on using magneto-resistance (MR) sensors to measure the DC component of the ion-beam. A detailed project plan was given in the last report (submitted on 30th of April 2015, see Table 1).

Table 1 Project Plan

No.	Milestone	Description	Status
1	**Testing existing GMR Sensors PCB**	Dismount of old Setup & General Inspection of HW	Completed
		Re-commissioning and tests with permanent magnet	
		Remount of PCB to the ring core	
		Comparative Hall-probe measurement (GMR)	
2	**Testing New TMR Sensors**	Purchase TMR Sensor	Completed
		Design and Realization of Test PCB for TMR	
		Comparative Hall-Probe measurement (TMR)	
3	**Open-loop N-DCCT Testing**	Application and measurements with DC wire signal	Completed
		Testing with GMR Sensors	
		Testing with TMR Sensors	
4	**Data Acquisition System Setup**	Learn DAQ interface SW	Completed
		Adapt the available DAQ SW at GSI for the N-DCCT	
		DC signal Readings	
		AC signal Readings	
5	**Noise Analysis for MR Sensors**	Theoretical Analysis for GMR and TMR noise	Completed
		Measurement of the sensors noise with the available PCB	
		Measurement of the noise PCB mounted to the toroidal with and without shielding	
		Usage of two sensors and re-measure the noise	
6	**Closed-Loop N-DCCT Design**	Electric Circuit Modeling on Cadence\ORCAD	Completed
		Theoretical Analysis	
		Software Modeling (using Simulink\MATLAB)	
		Search/buy external missing components	
		Realization of Closed-loop PCB	

The plan described the project's milestones: Testing the existing hardware of the N-DCCT, investigating the characteristics of new MR sensor types, designing a closed-loop N-DCCT and setting up specialized DAQ for the device readings. Up to 31st of December 2014, testing of the existing hardware

and setting up the DAQ were completed. The study of new MR sensors and design of the closed-loop N-DCCT were done theoretically. In specific, the MR sensors theoretical noise characteristic was studied but without practical measurements. Also, the closed-loop N-DCCT device was theoretically designed but by then no practical testing had been employed. In this report, detailed description of practical measurements for these milestones is presented. In addition, future work of the project is discussed at the end of the report.

- **Noise Analysis of MR Sensors**

In order to measure the current resolution of the proposed N-DCCT, theoretical and practical studies for the MR sensors noise characteristics were done. The theoretical study was presented in the last project report. The conclusion of this study showed that Tunneling MR (TMR) sensors would exhibit more noise compared to Giant MR (GMR) sensors. Also it introduced a performance evaluation parameter for the MR sensors called "Detectivity Factor". It is defined as the ratio between the noise output voltage (at a given frequency) and the sensitivity of the MR sensor. A low "D Factor" means that the sensor is more suitable for low magnetic field applications. This factor can be calculated by the following equation:

$$D = \frac{\sqrt{S_V}}{R_{BV}}$$

where 'D' is the sensor's Detectivity in [mT/√Hz], '$\sqrt{S_V}$' is the noise output voltage of the sensor at a given frequency in [V/√Hz], 'R_{BV}' is the sensor's sensitivity [V/mT]

Though the TMR noise is higher than the GMR, the value of its "D Factor" is lower. This is attributed to the fact that the TMR sensor has higher sensitivity. Noise measurements of MR sensors were carried out at GSI. The measurements were done using LeCroy Oscilloscope with 12-bit resolution and a Fast Fourier Transform feature. Two measurement setups were prepared for that purpose. The MR sensors are soldered on dedicated PCBs. These boards were implemented for the open-loop N-DCCT.

In the first setup, each MR sensor PCB is placed inside a cylindrical electro-magnetic shield box. The noise output voltage is measured while no external field is applied. The voltage supply is turned off and on to record the noise in both cases. This is done to study the effect of the biasing current. Four MR sensor models were tested: the GMR sensor "NVE AA002" and TMR sensors "45F, 57F-SOP8 and 57F-DFN". Since our main concern is to measure the DC component of the ion-beam, the value of the output voltage noise power spectral density at DC and low frequencies is measured. The sensor that showed the lowest noise was the TMR57F-DFN and the highest was the TMR45F sensor.

Table 2 summarizes the first test measurements. The output voltage noise is calculated for a standard 50Ω load. Figs. 1, 3, 5 and 7 show the output voltage noise power spectral density -while the supply is turned off- for the GMR sensor and TMR sensors (45F, 57F-SOP8 and 57F-DFN) respectively. TMR and GMR sensors are biased at 5V and ±8V respectively. Figs. 2, 4, 6 and 8 show the output voltage noise -while the supply is turned on- with the same order. The TMR45F model has the highest output voltage

noise. This is attributed to the fact that it has the highest internal resistor value and sensitivity [1]. Turning the biasing on will cause noise resonance at high frequencies. This resonance is triggered by magnetic thermal noise [2].

Table 2 Output Voltage Noise Measurements at DC using Electro-magnetic Shield

Sensor Type	Output Voltage noise at DC (Biasing ON)	Output Voltage noise at DC (Biasing OFF)	Resistance (kΩ)	Datasheet Sensitivity (mV/V/Oe)
TMR 57F DFN8	-88.8dBm	-88dBm	45	4.9
GMR AA002	-84.26dBm	-125.9dBm	5	3 - 4.2
TMR 57F SOP8	-81.53dBm	-98.16dBm	90	4.9
TMR 45F SOP8	-61.99dBm	-91.85dBm	80	12

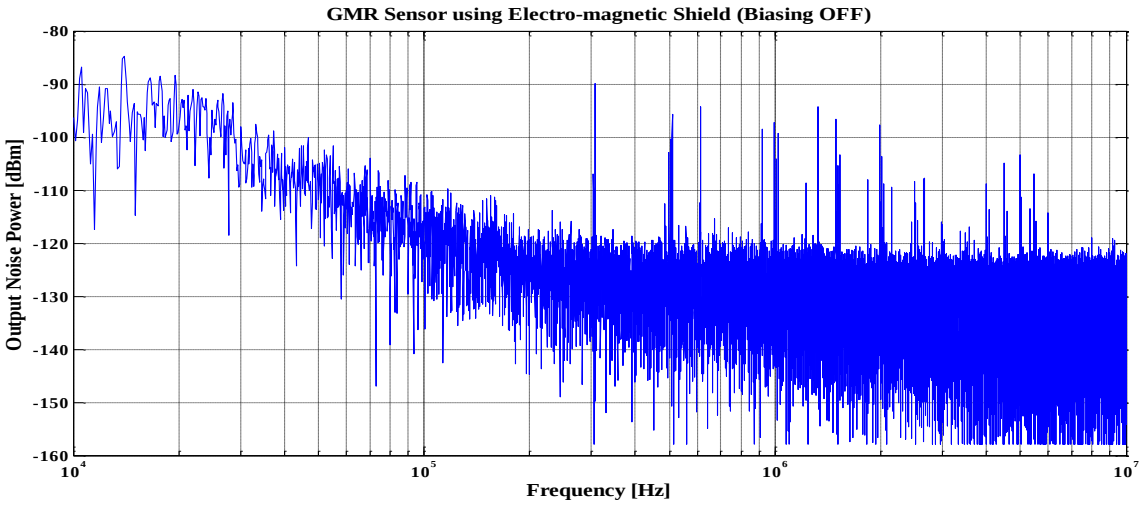

Figure 1 GMR Sensor Output Noise Power Spectrum (Biasing OFF)

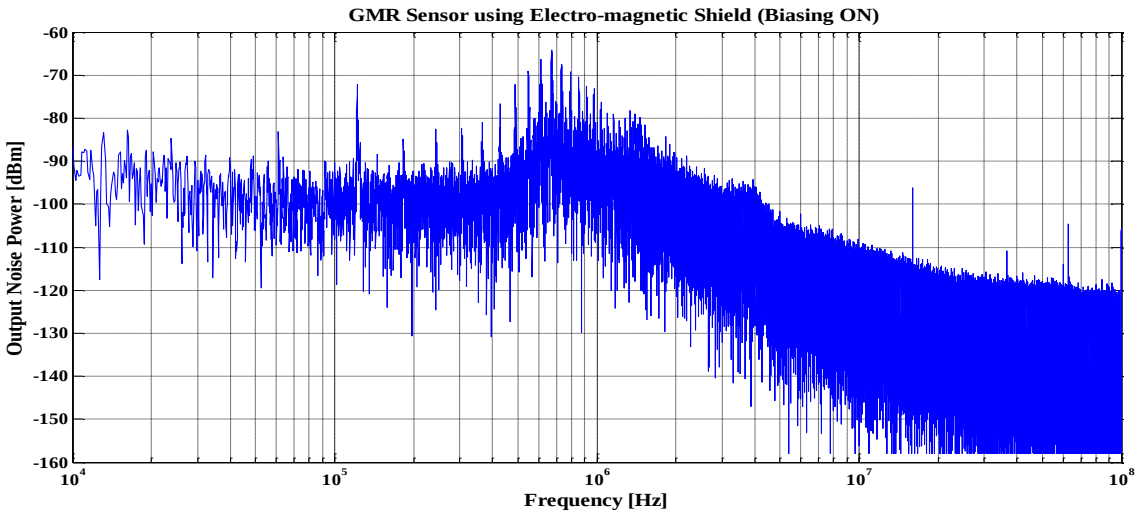

Figure 2 GMR Sensor Output Noise Power Spectrum (Biasing ON)

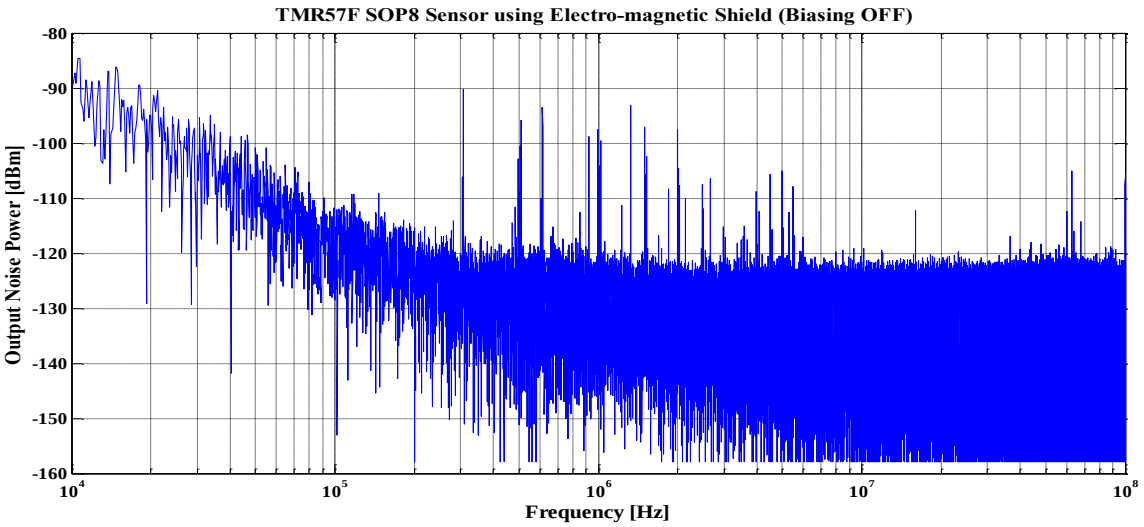

Figure 3 TMR57F-SOP8 Sensor Output Noise Power Spectrum (Biasing OFF)

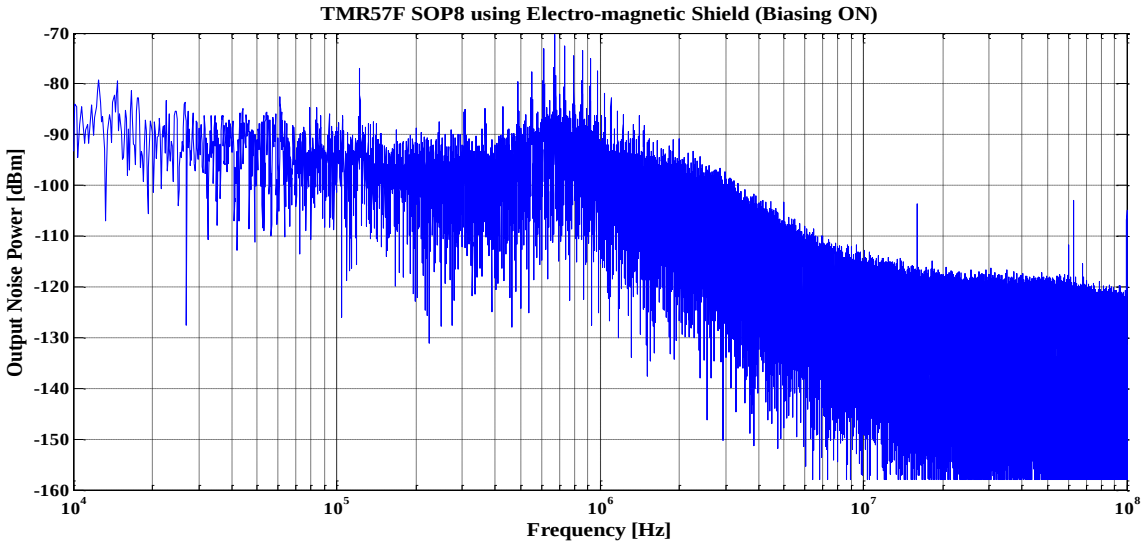

Figure 4 TMR57F-SOP8 Sensor Output Noise Power Spectrum (Biasing ON)

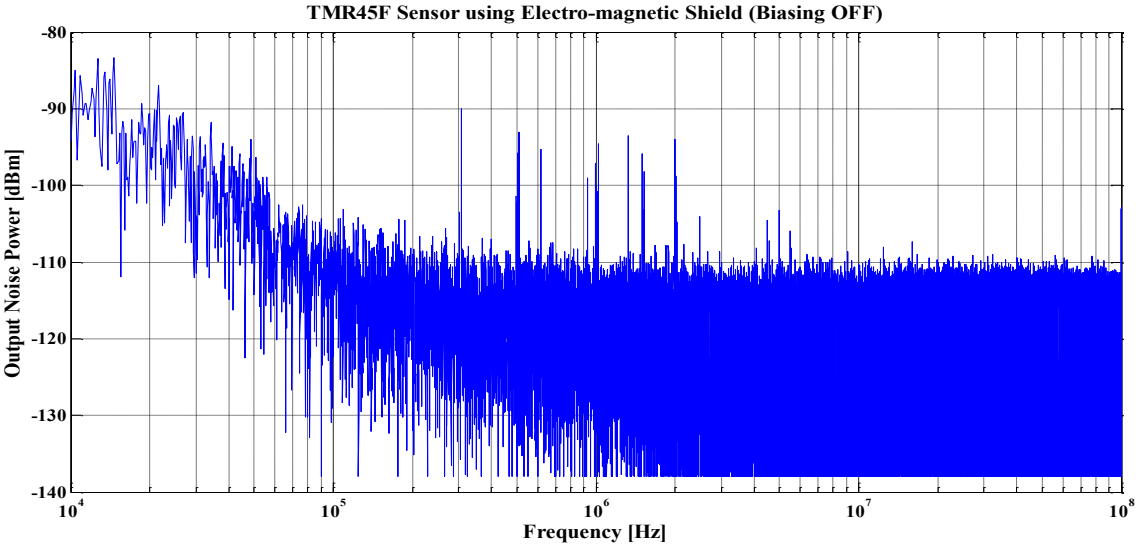

Figure 5 TMR45F Sensor Output Noise Power Spectrum (Biasing OFF)

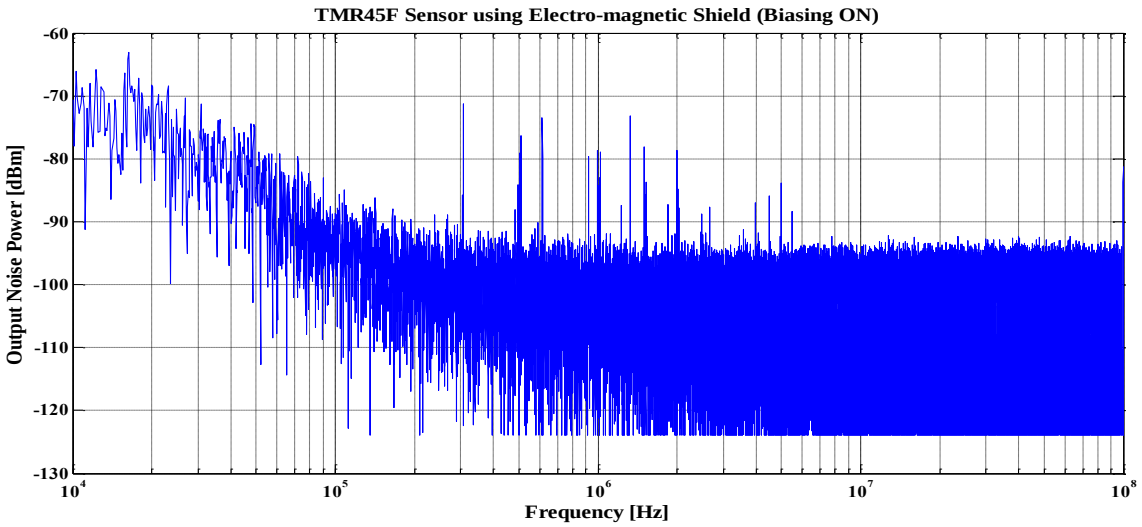

Figure 6 TMR45F Sensor Output Noise Power Spectrum (Biasing ON)

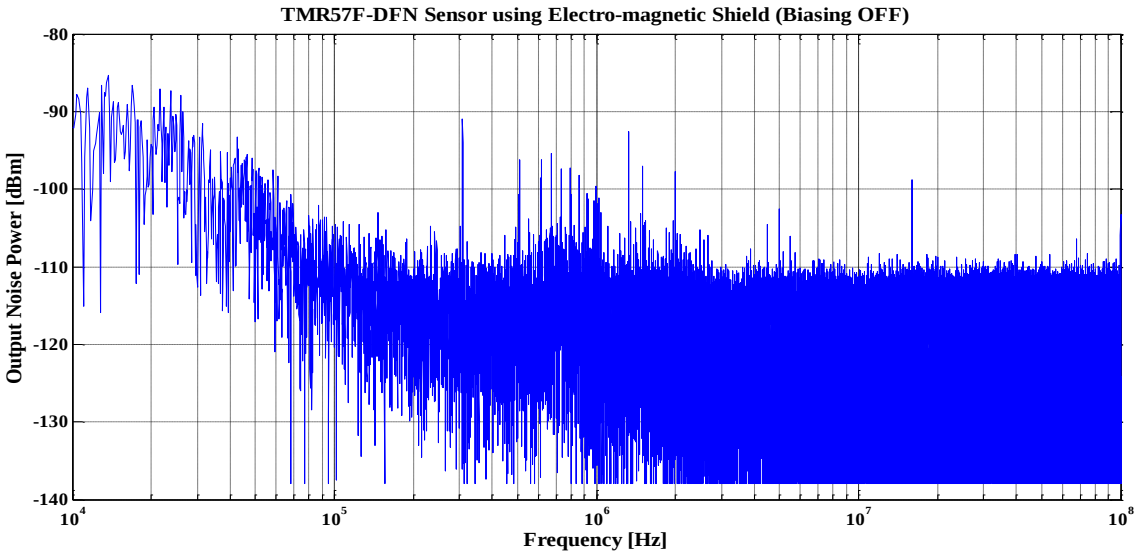

Figure 7 TMR57F-DFN8 Sensor Output Voltage Noise Spectrum (Biasing OFF)

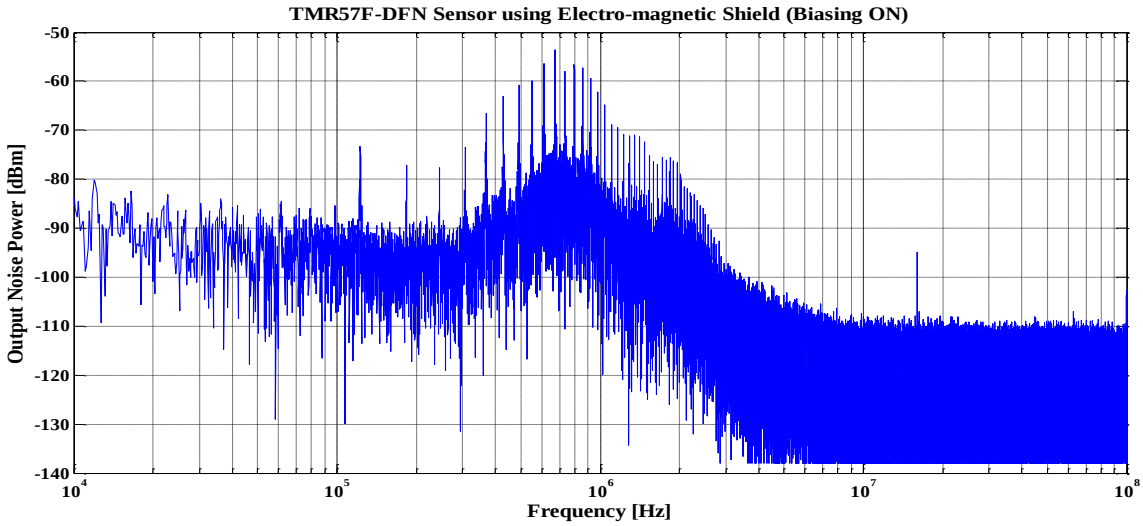

Figure 8 TMR57F-DFN8 Sensor Output Voltage Noise Spectrum (Biasing ON)

The second noise measurement setup is done to calculate the open-loop N-DCCT "D Factor". In this measurement setup, the MR sensor PCB is placed inside the air gap of the ring core. The air gap width is for SOP8 and DFN8 sensors were 10mm and 5mm respectively. However, both the upper and lower gaps are used. Thus, a differential output voltage is measured. To calculate the "D Factor", both the signal and noise output voltage signals are measured. The magnetic field density in the air gap and the differential output voltage of the open-loop N-DCCT is given by:

$$B_{gap} = \frac{\mu_o}{d} I_{beam}$$

$$V_{out} = V_{Sensor1} - V_{Sensor2} = 2A_v R_{BV} B_{gap}$$

where 'B_{gap}' is the magnetic field intensity inside the air gap [mT] and 'I_{beam}' is the ion-beam current [A], 'μ_o' is the vacuum permeability [T.m/A], 'd' is the air gap width [m], 'A_v' is the PCB voltage amplifier gain (10V/V) and 'R_{BV}' is the MR sensor's sensitivity [V/mT]

Our main concern is to measure the value of the noise signal at low frequencies, particularly at DC. The sensor that showed the lowest noise was the TMR57F-DFN and the highest noise was measured from the TMR57F-SOP8 sensor. Table 3 summarizes open-loop N-DCCT noise measurements at DC.

To simulate the effect of the ion-beam current, a wire carrying DC current is placed at the center of the ring core. The complete setup is placed inside a metallic box for shielding as shown in Fig. 9. It is worth mentioning that the GMR and TMR sensor's PCB is supplied using ±8V and 5V voltage supply respectively. To improve comparability, the output signal of the GMR sensor is scaled such that both sensors would have the same voltage supply value. Table 4 gives the open-loop N-DCCT measured sensitivity, output noise, "D Factor" and minimum detectable current (calculated from the basic equation of the N-DCCT). The TMR57F-DFN8 and TMR45F sensors have better resolution compared to other models. In the following, detailed measurement figures for both the output voltage signal and noise spectrum are given (Figs. 10-17).

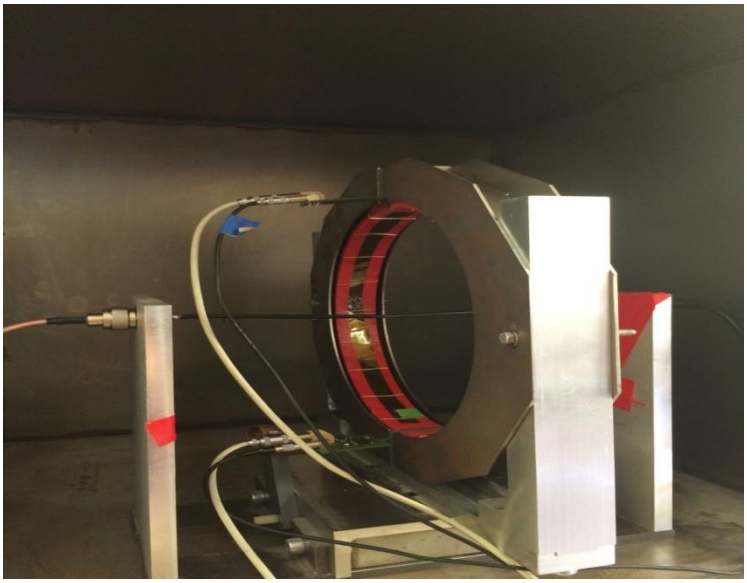

Figure 9 Open-loop N-DCCT Measurement Setup

Table 3 Noise Measurement at DC (Differential Sensors)

Sensor Type	Output Voltage noise at DC
TMR 57F DFN8	-71.06dBm
GMR AA002	-68.97dBm
TMR 45F SOP8	-61.1dBm
TMR 57F SOP8	-55.89dBm

Table 4 Measured Specs of the MR based Open-loop N-DCCT

Sensor Type	N-DCCT Sensitivity [V/A]	Output Noise at low frequency [µV/√Hz]	Detectivity [nT/√Hz]	Minimum Detectable Current at DC [µA]
GMR AA002	0.396	80	25.31	202.24
TMR 45F	1.56	200	16.03	128
TMR 57F (DFN)	1.044	65	15.57	62.28
TMR 57F (SOP)	0.794	359	56.5	452.1

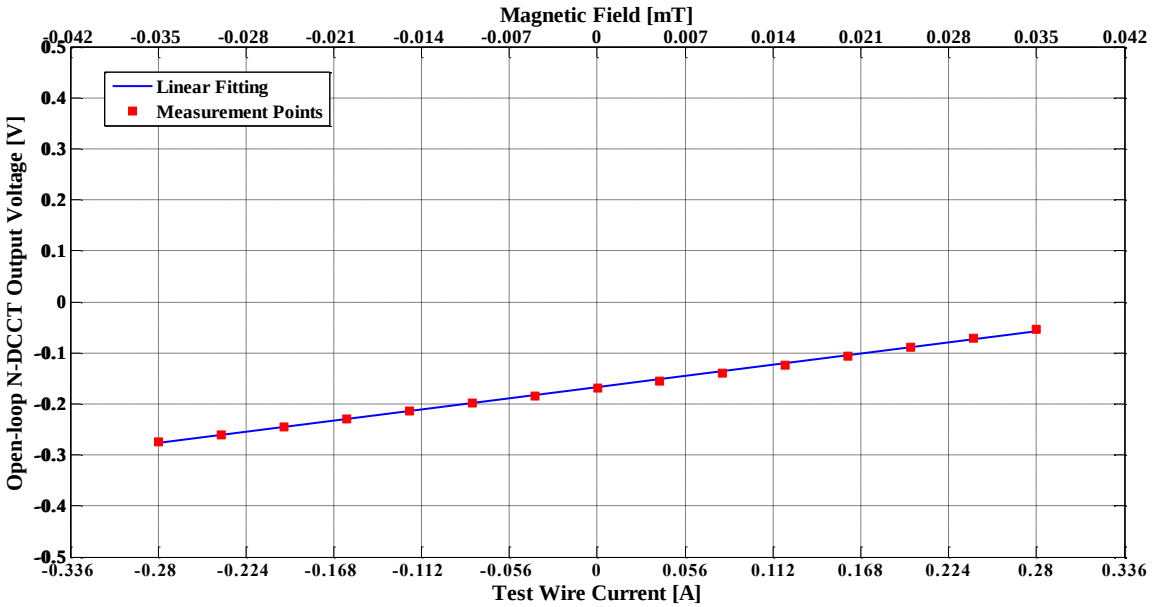

Figure 10 Open-loop N-DCCT Output Voltage vs. Input Current (GMR AA002)

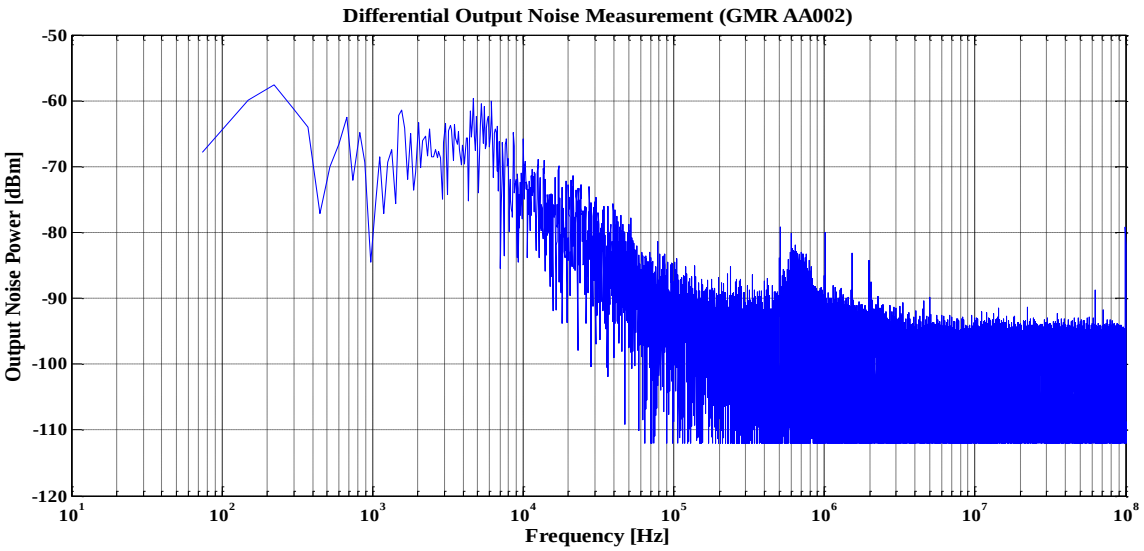

Figure 11 Differential Output Noise Frequency Spectrum (GMR AA002)

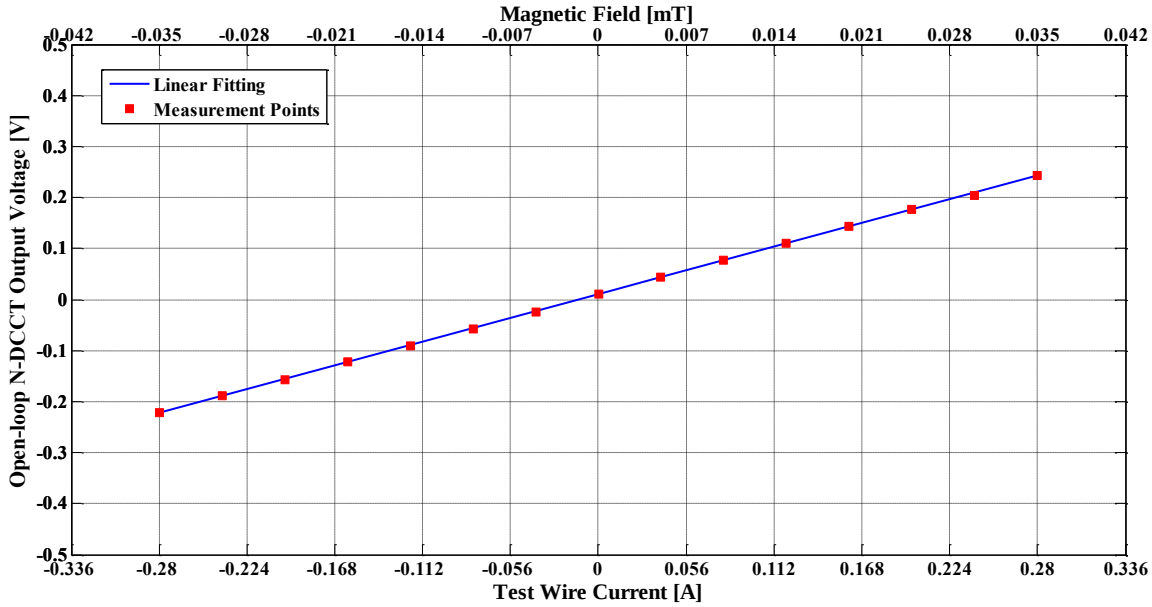

Figure 12 Open-loop N-DCCT Output Voltage vs. Input Current (TMR57F-SOP8 Sensor)

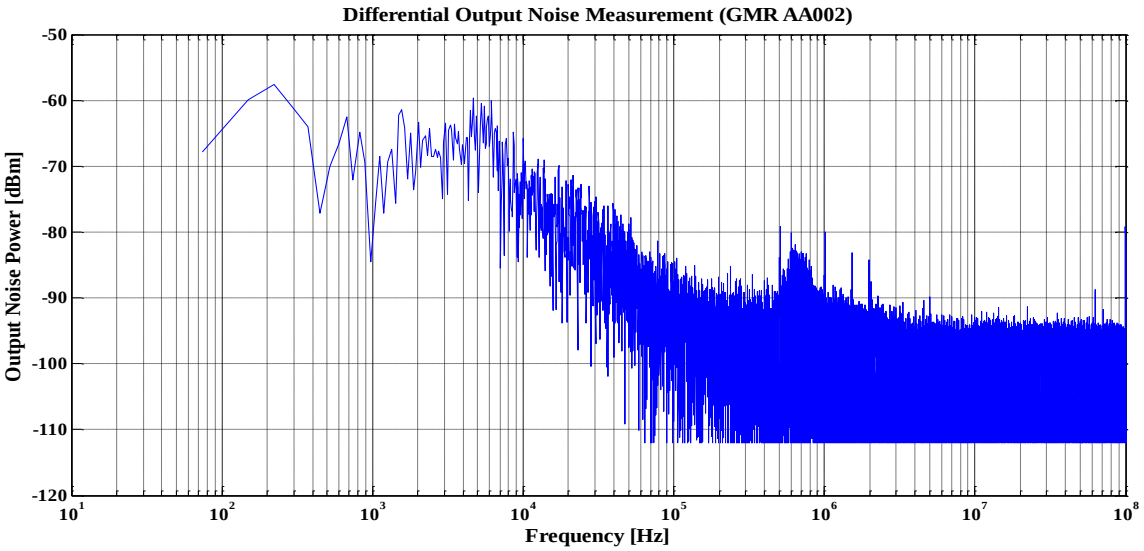

Figure 13 Differential Output Noise Spectrum (TMR57F-SOP8)

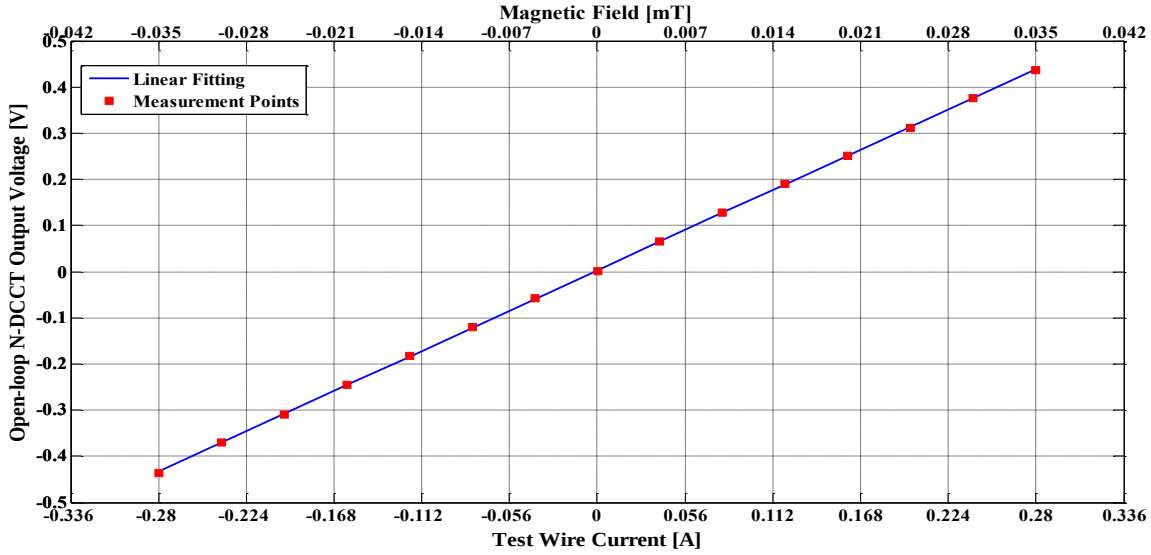

Figure 14 Open-loop N-DCCT Output Voltage vs. Input Current (TMR45F)

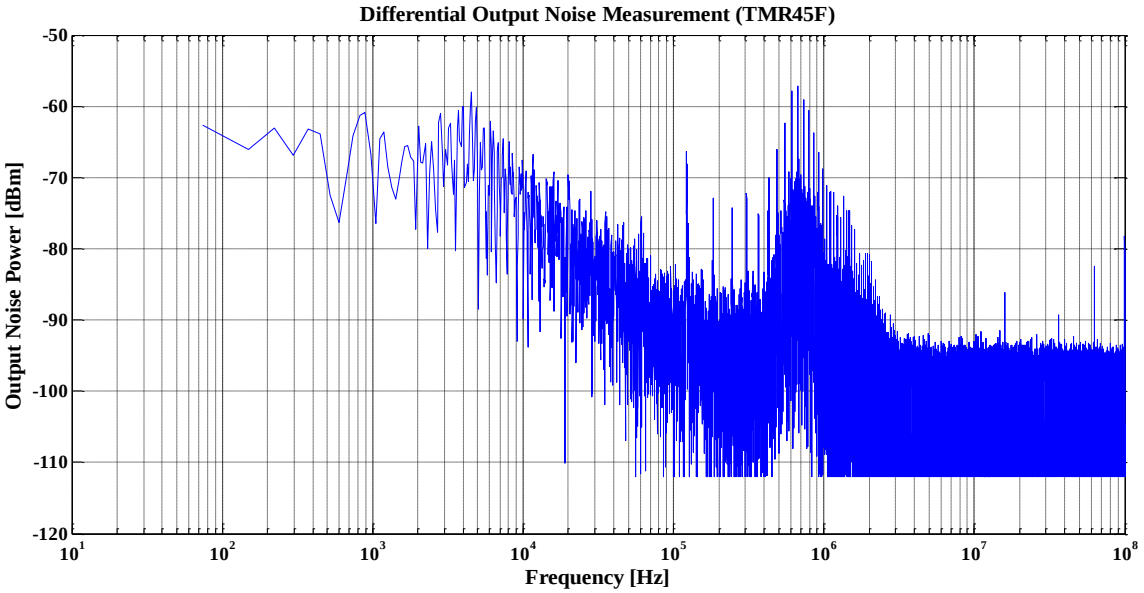

Figure 15 Differential Noise Power Spectral Density Measurement (TMR45F)

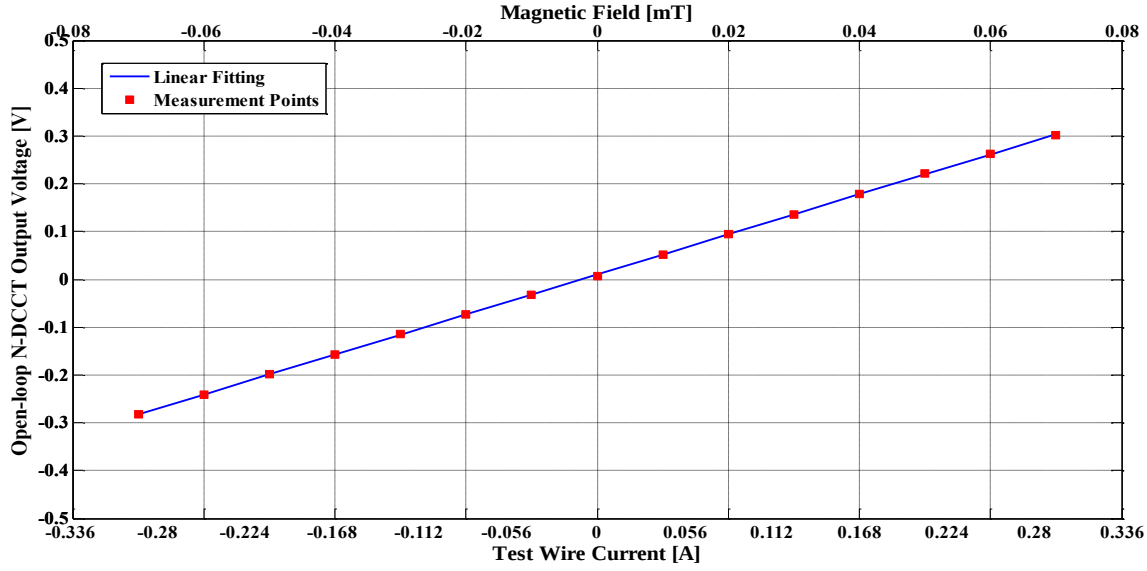

Figure 16 Open-loop N-DCCT Output Voltage vs. Input Current (TMR57F-DFN8)

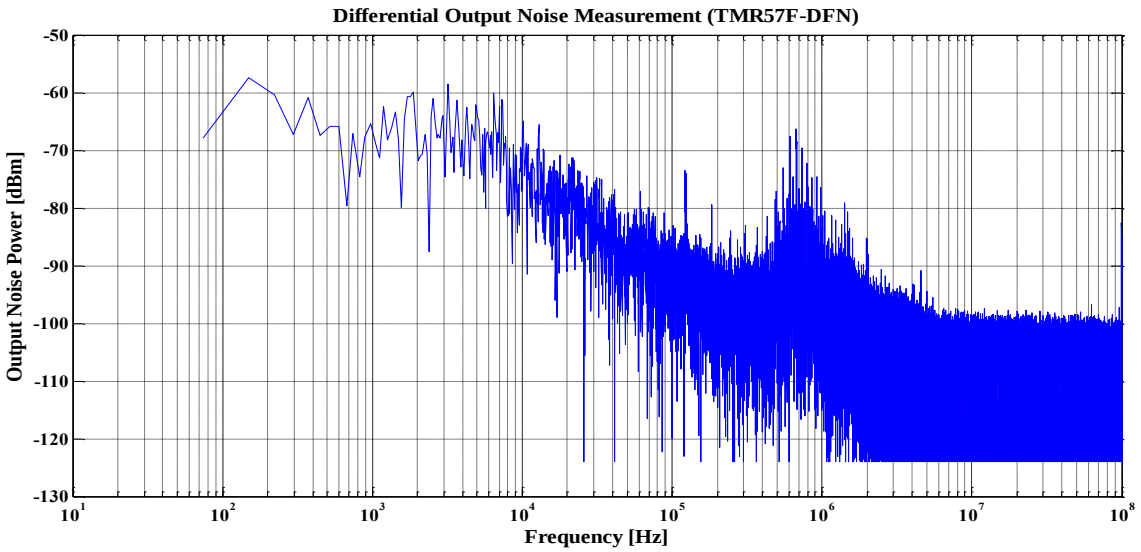

Figure 17 Differential Output Noise Spectrum (TMR57F-DFN8)

❖ Closed-loop N-DCCT Hardware Implementation

To improve the linearity and sensitivity of the N-DCCT, a feedback loop was designed. The objective is to deliver a feedback current that cancels the magnetic field of the ion-beam inside the air gap. This measurement principle is called "Zero-flux" and it is currently used in commercial DCCT. The theoretical design of the feedback loop was presented in the last project report. By adding the feedback loop, the N-DCCT device becomes a closed-loop one. Fig. 18 shows the proposed design of the device.

A second PCB is designed to convert the voltage signal of the open-loop N-DCCT to a feedback current "I_{FB}" using Operational Transconductor Amplifier (OTA). The feedback current flows in "N" turns winding wire terminated with a resistive load. The voltage across the resistive load "R_L" gives a direct measure of the ion-beam current "I_{beam}". The feedback current and output voltage of the closed-loop N-DCCT is given by:

$$I_{beam} = -NI_{FB}$$

$$V_{FB} = R_L I_{FB} = -\frac{R_L}{N} I_{beam}$$

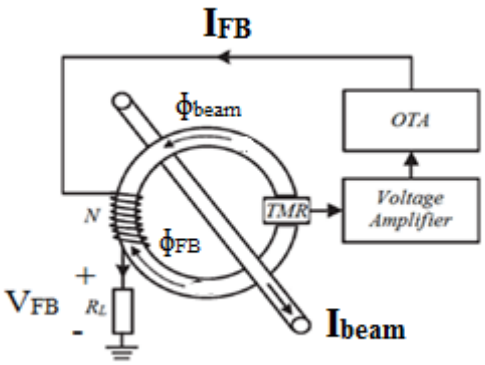

Figure 18 Proposed Closed-loop N-DCCT Structure

The PCB layout for the closed-loop N-DCCT is shown in Fig. 19. It consists of four OTAs that transform the open-loop N-DCCT output voltage to a feedback current. Multiple parallel OTAs are used to enhance the overall dynamic range of the N-DCCT. Commercial OTAs from Texas Instruments were used (OPA860 and OPA861). They have the same transconductance gain but they have different input dynamic ranges and noise characteristics. Both OTA models are tested; their output voltage and noise are measured. Fig. 20 shows the fabricated PCB of the closed-loop N-DCCT.

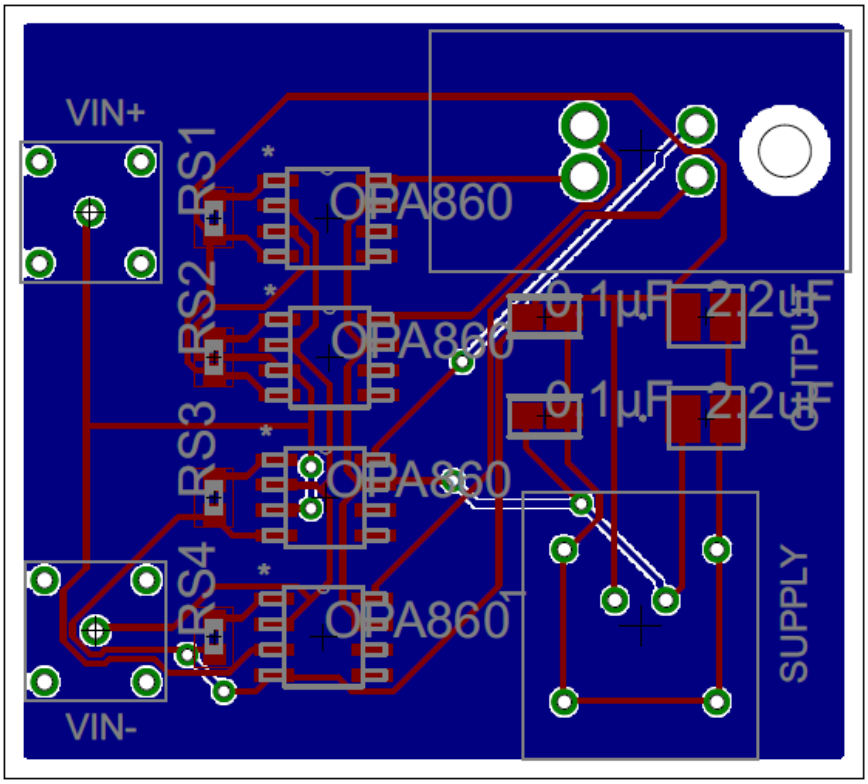

Figure 19 Feedback Loop PCB Board Layout

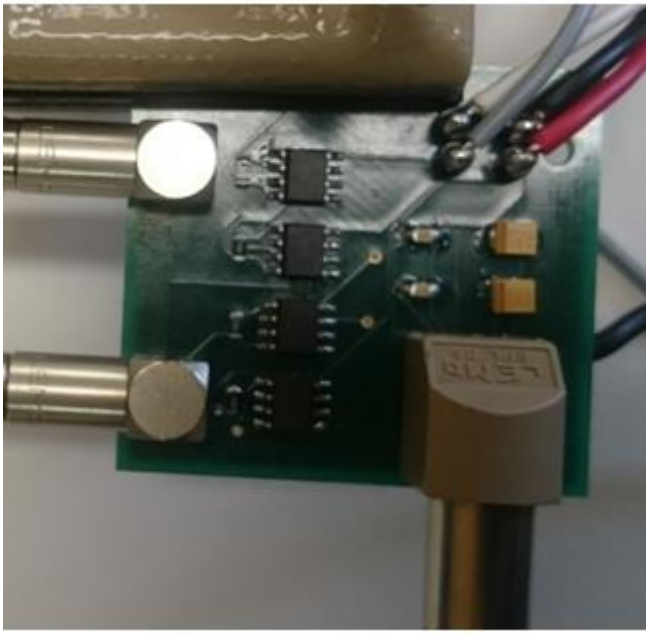

Figure 20 Fabricated Feedback Loop PCB

1. OTA Signal-to-Noise Ratio Calculation

To calculate the Feedback loop SNR, the noise characteristic of the OTAs used is theoretically studied. The OTA noise sources are intrinsic ones such as: the thermal, shot and flicker type. The OTAs have differential input ports, thus they can be modeled using the classical two port network noise model shown in Fig. 21. The input voltage 'v_i' and current 'i_i' noise sources depend on the internal structure of the circuit. The output voltage noise of one OTA is given by the following equation:

$$V_0 = \sqrt{\left[2\overline{v_i^2} + R_S^2\overline{i_i^2} + 4kTR_S\right]\left[\frac{R_L}{R_G + \frac{1}{g_m}}\right]^2 + \left[R_G^2\overline{i_i^2} + 4kTR_G\right]\left[\frac{R_L}{\frac{1}{g_m}}\right]^2}$$

Where "R_S" and "R_G" are the source resistances of the positive and negative terminals respectively, "g_m" is the OTA transconductance gain, 'k' is Boltzmann's constant, 'T' is temperature in Kelvin and "R_L" is the load resistance

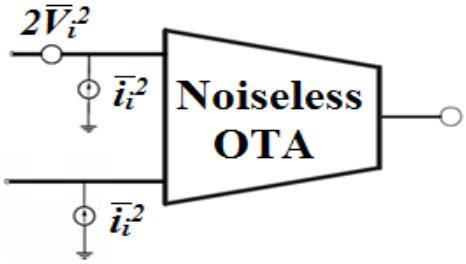

Figure 21 Differential OTA Noise Model

Before measuring the noise of the OTAs, the PCB functionality was tested. The supply voltage used for the OTAs was ±5V. The OTA differential input was connected to a signal generator. The output node was connected to a 5kΩ resistor load. The input voltage of the OTAs was set to a sinusoidal signal at 1 kHz and 80mVpp amplitude. Both the output voltage of the OTA was measured as well as the noise spectrum. The results are shown in Figs. 22 and 23 for single OTA model OPA860.

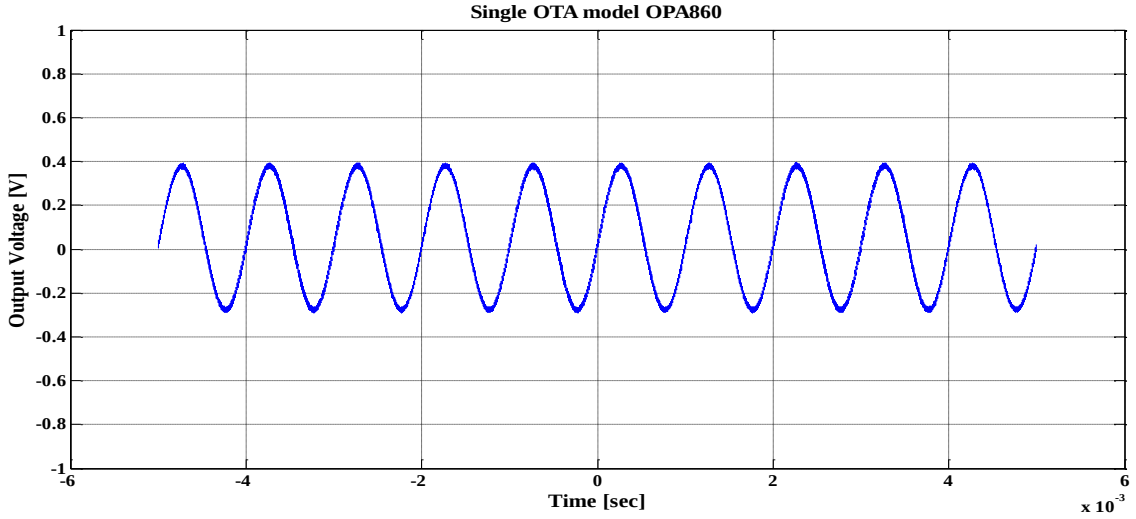

Figure 22 Measured Output Voltage (Single OPA860)

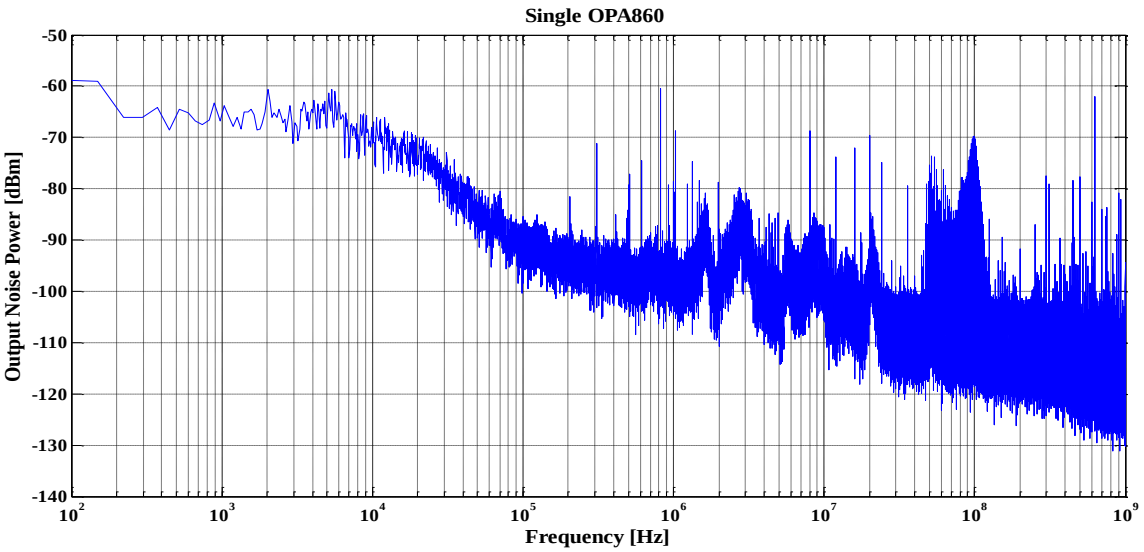

Figure 23 Measured Noise Spectrum (Single OPA860)

The output voltage and noise spectrum of a single OTA OPA861 are shown in Figs. 24 and 25 respectively. The output voltage is 688mVpp and 728mVpp for the models OPA860 and OPA861 respectively. The output noise power spectral density at DC is -63.76dBm and -45.23dBm for OPA860 and OPA861 respectively.

Since the ion beam current is in the range of few Milli-Amperes to Amperes, a large number of turns are needed. However, this will cause the parasitic elements to increase and may lead to unstable system. Thus, multiple OTA circuits are used (‘m’ OTAs) to increase the magnitude of the feedback current. Four OTAs were used and tested under the same conditions. The output voltage and noise spectrum of four parallel OPA860 is shown in Figs. 26 and 27 respectively. The noise at low frequencies was less in case of four OTAs in parallel compared to using only one. This is attributed to the fact that the output voltage noise is scaled with the factor “1/sqrt (m)” [3]. The PCB output voltage for OPA860 model is 1.81Vpp and the output noise power spectral density at DC is -73.02dBm.

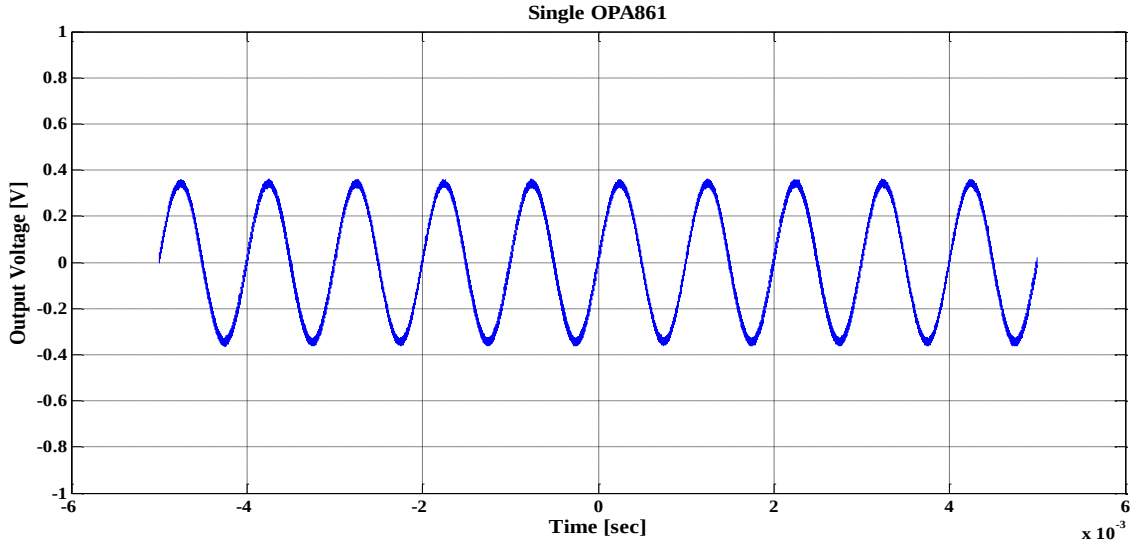

Figure 24 Measured Output Voltage (Single OPA861)

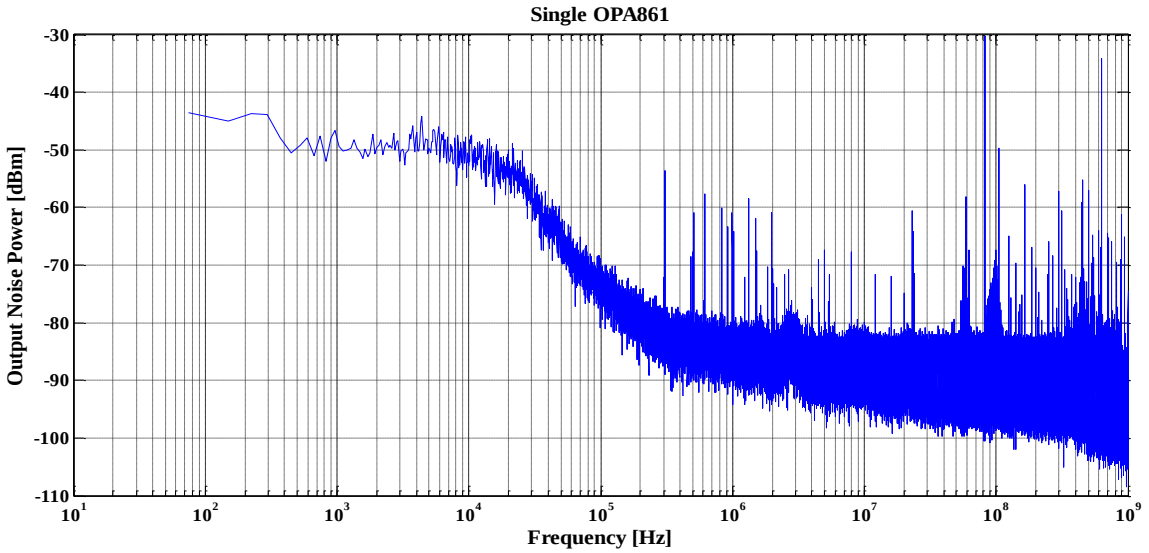

Figure 25 Measured Noise Spectrum (Single OPA861)

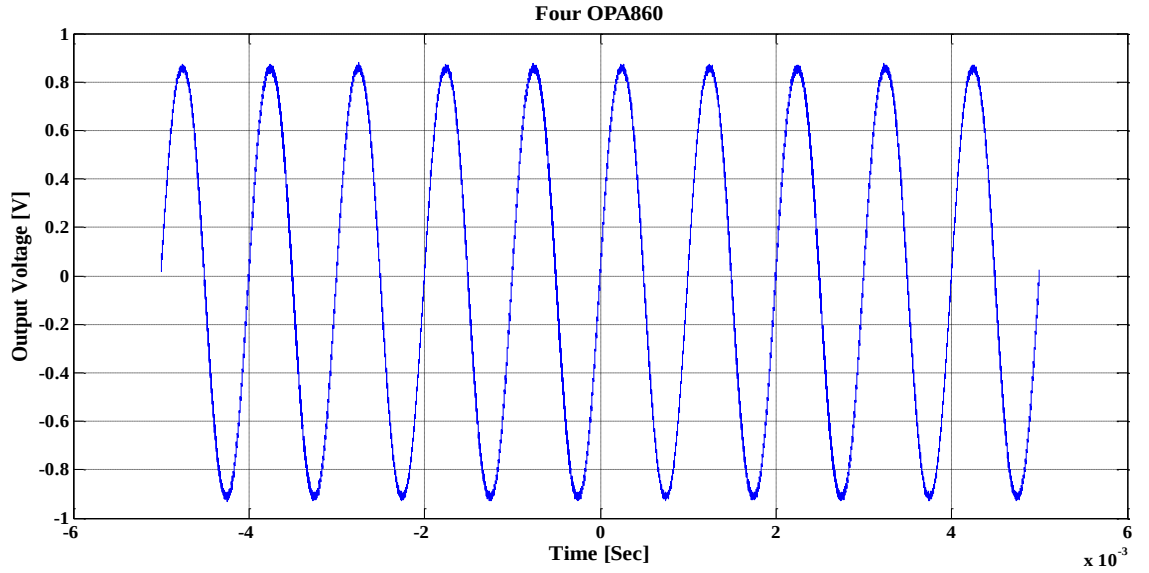

Figure 26 Measured Output Voltage (Four OPA860)

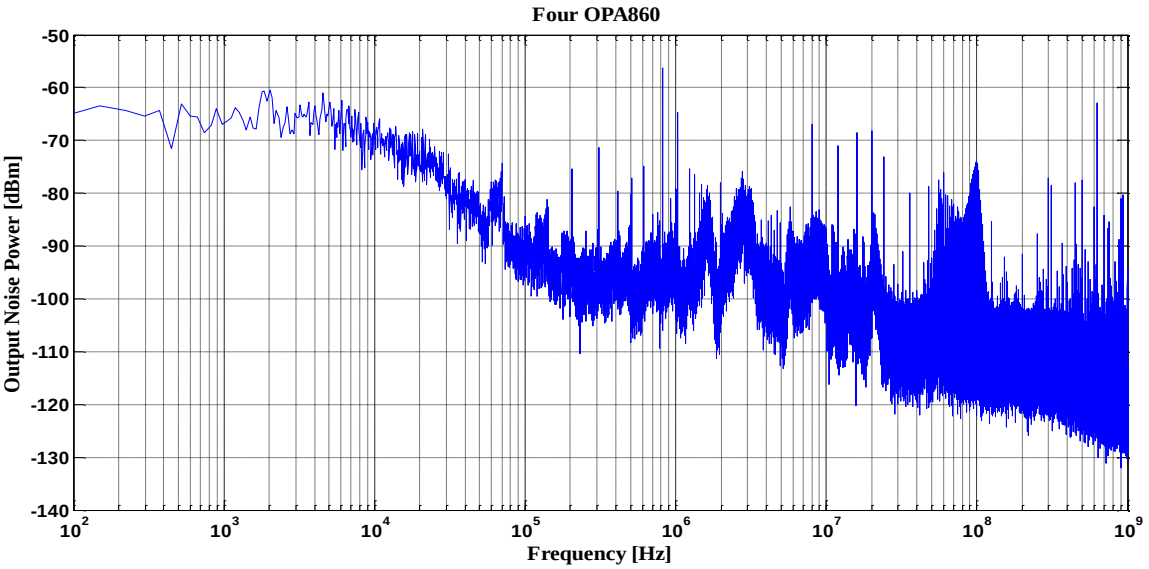

Figure 27 Measured Noise Spectrum (Four OPA860)

The output voltage and output noise voltage spectrum of four parallel OPA861 is shown in Figs. 28 and 29 respectively. The PCB output voltage for OPA861 model is 1.9Vpp and the output noise power spectral density at DC is -55.83dBm. The signal to noise ratio for the OTA models is summarized in Table 5.

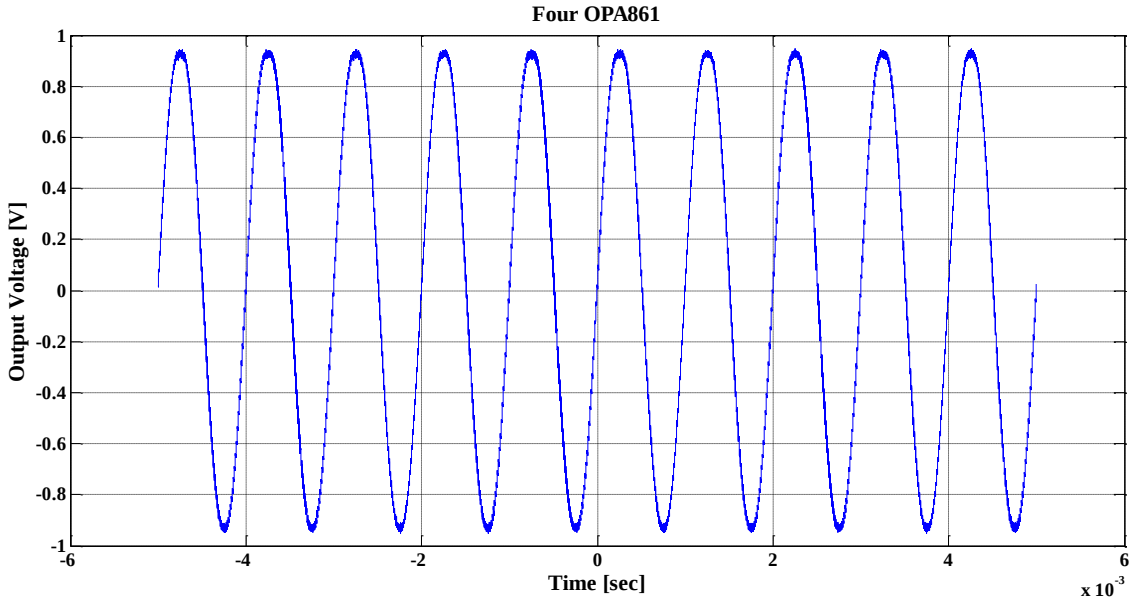

Figure 28 Measured Output Voltage (Four OPA861)

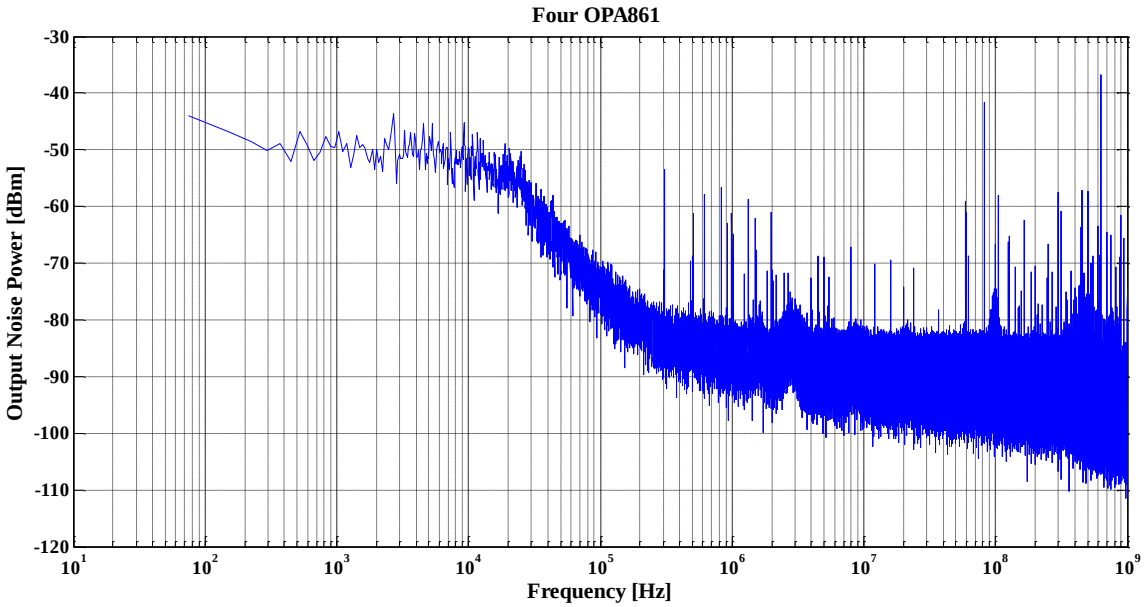

Figure 29 Measured Noise Spectrum (Four OPA861)

Table 5 Signal-to-noise Ratio for the Closed-loop PCB

OTA Model and Number	OPA860	OPA861
One	73.52dB	55.48dB
Four	91.18dB	74.41dB

2. Feedback Loop Measurements

The design of the closed-loop N-DCCT was implemented using commercial ICs. To check the system stability, the transfer function of the system was derived theoretically and simulated using MATLAB. A test setup was prepared at GSI using the same equipment shown in Fig.9, while adding 'N' windings and 'R_L' resistive load. The value for 'N' and 'R_L' was set at 50 and 620Ω respectively. Four OTAs were used and they are biased using ±5V voltage supply. Since the OTA has a differential input, two TMR sensors were used for this test. The sensors were placed in the upper and lower air gaps of the ring core.

An offset current is introduced to the system to cancel the remanence effect such that the OTA input terminals have the same common mode value. In this test, TMR45F sensors were used. The offset current value was set at 256mA. The common mode voltage at the OTA's input terminals was set at -1V and their differential voltage is zero.

Since the OTA positive and negative input resistances are not the same, the DC gain of the closed-loop system was re-derived using circuit analysis. The exact DC gain of the closed-loop N-DCCT after taking into consideration the non-idealities and parasitics of the electronics circuits used in the system is given by:

$$I_{FB}(S=0) = -\frac{mG_{mo}R_{out2}R_{BV}A_{vo}\left(R_zR_{in2} - R_yR_{in3}\right)}{NmG_{mo}R_{out2}R_{BV}A_{vo}\left(R_zR_{in2} - R_yR_{in3}\right) + R_xR_yR_z} I_{beam}$$

$$R_x = mR_L + R_{out2}$$

$$R_y = mR_{out1} + R_{in2}$$

$$R_z = mR_{out1} + R_{in3}$$

where "G_{mo}" is the OTA's transconductance gain [A/V], "R_{out2}" is the OTA's output resistance [Ω], "R_{in2}" is the OTA's positive terminal intput resistance [Ω], "R_{in3}" is the OTA's negative input resistance [Ω] and "R_{out1}" is the voltage amplifier's output resistance [Ω]

Assuming $NmG_{mo}R_{out2}R_{BV}A_{vo}\left(R_zR_{in2} - R_yR_{in3}\right) \gg R_xR_yR_z$, the feedback current can be approximated to the value of:

$$I_{FB} \cong -\frac{1}{N} I_{beam}$$

The step response of the feedback current was simulated using MATLAB using the value for 'N=50'. The value of the transfer function parameters (from Datasheets) are given in Table 6. The result is shown in Fig. 30 for different number of OTAs connected in parallel. The values of the parameters taken from the datasheet are subject to temperature change. The voltage op-amp parameters are calculated based on the 3-dB BW given in the datasheet. The step response of the closed-loop N-DCCT output voltage was also measured while having an input voltage as a square wave of 2Vpp amplitude (test wire current peak-

to-peak of 320mA), 1.6V offset and 1 kHz frequency. The result is shown in Fig. 31 and 32 for the OTA model OPA860 and OPA861 respectively. The system is stable from simulation and measurement results.

Table 6 Values of the Parameters used for the Closed-loop N-DCCT

Parameter	Value	Parameter	Value
N	50	m	4
$\mathbf{R_L}$	620Ω	R_{out1}	8Ω
$\mathbf{R_{in2}}$	455kΩ	R_{in3}	10.5Ω
$\mathbf{R_{out2}}$	54kΩ	G_{mo}	95mA/V

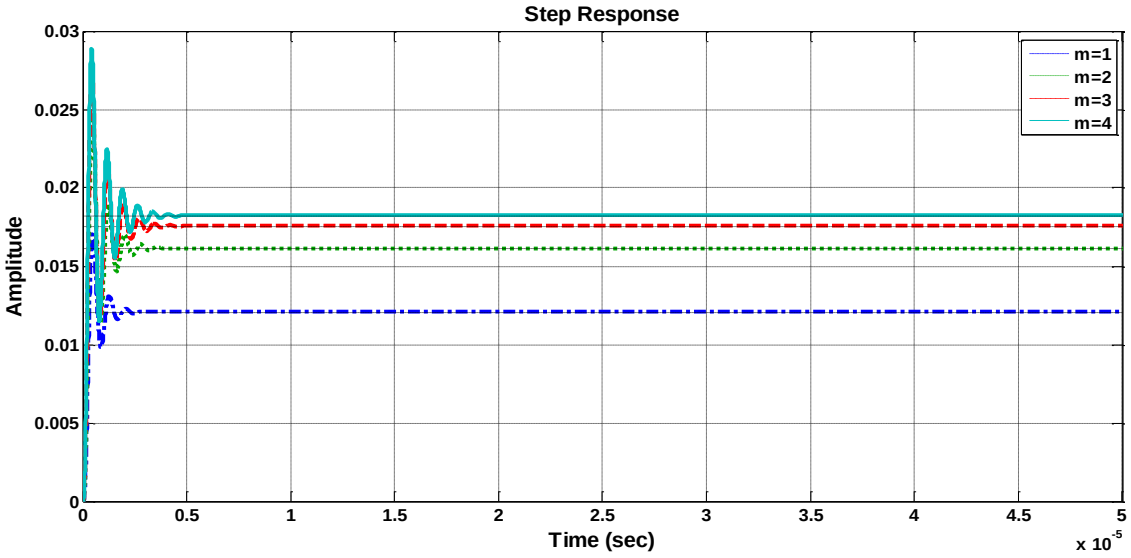

Figure 30 Step Response of the Closed-loop System feedback Current using MATLAB (m=no. of used OTAs)

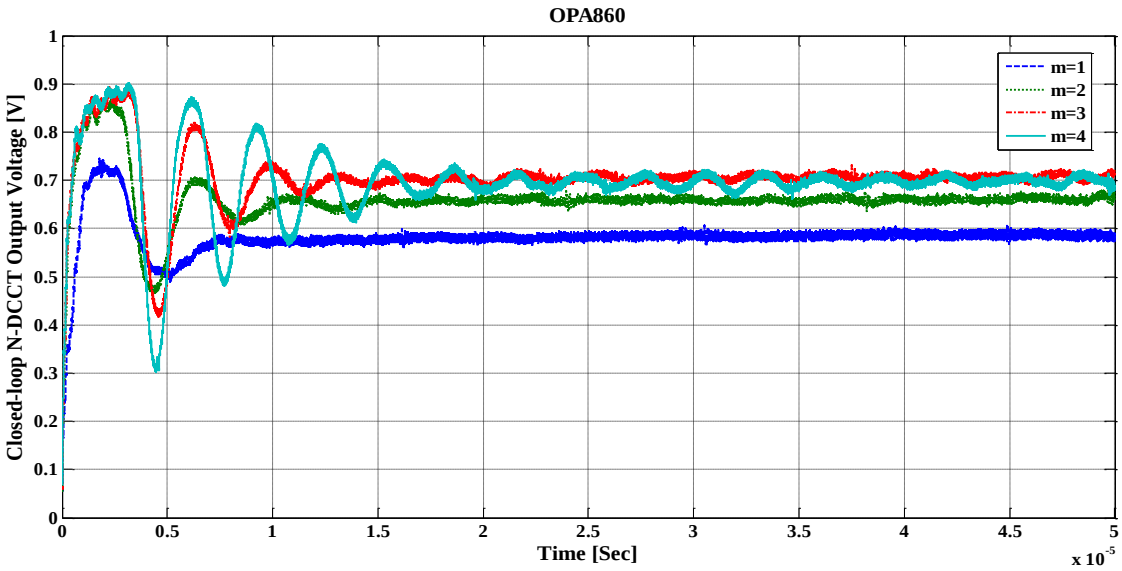

Figure 31 Step Response of the Closed-loop N-DCCT Output Voltage (OPA860, m=no. of used OTAs)

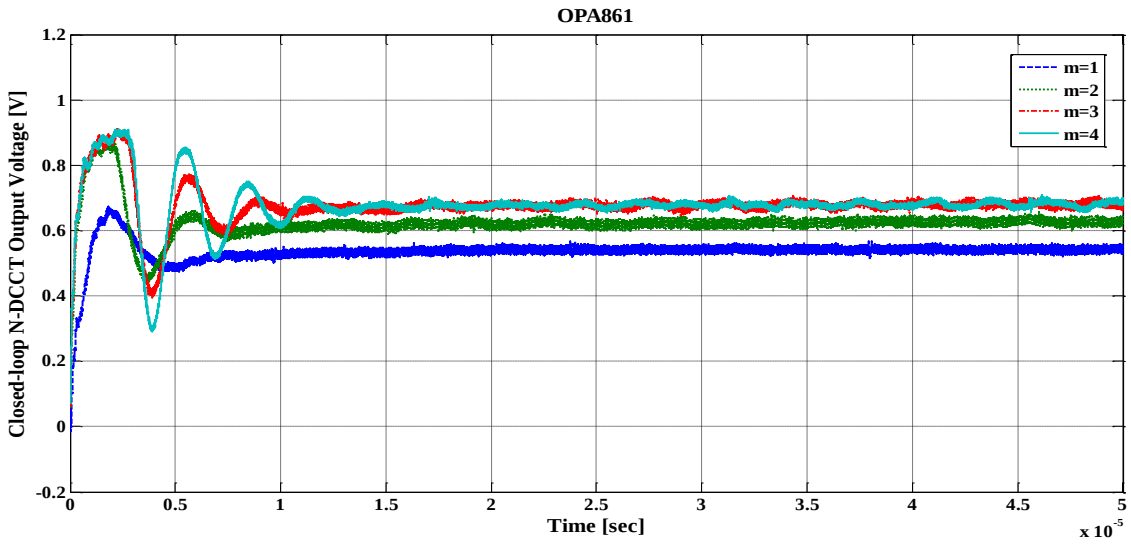

Figure 32 Step Response of the Closed-loop N-DCCT Output Voltage (OPA861, m=no. of used OTAs)

Further tests were done for the feedback system including application of sinusoidal and ramp signals with the same specifications as the square wave signal mentioned above while varying the signal's amplitude. Both OTA models show the same results. The output voltage for OPA860 while applying input signal with different amplitudes is shown in Figs. 33 and 34 for sinusoidal and ramp signals respectively.

The output voltage of the closed-loop N-DCCT was also measured while introducing a DC voltage signal with an offset 1.6V. The DC offset was varied from 0.4V to 2.8V and this corresponds to a DC current changing from 0.064A to 0.448A. The output voltage is shown in Figs. 35 and 36 for the OTA model OPA860 and OPA861 respectively. The theoretical sensitivity for the closed-loop N-DCCT is calculated based on the ICs parameters given in the datasheet. The value of the "D Factor" for the closed-loop N-DCCT is calculated from the noise measurement.

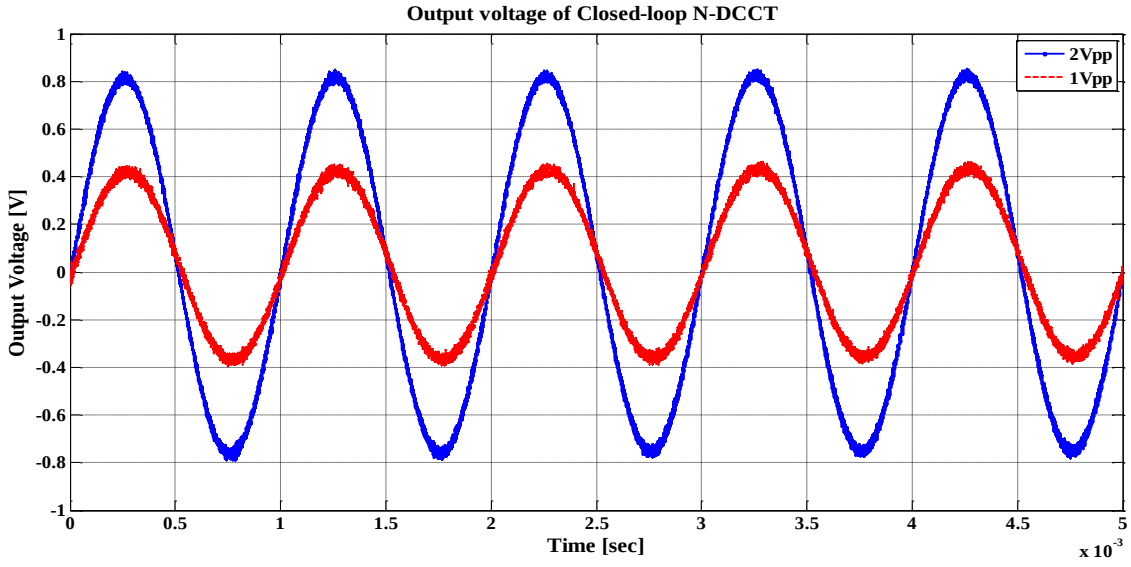

Figure 33 Closed-loop N-DCCT Output Voltage with Sinusoidal Input Signal (Four OPA860)

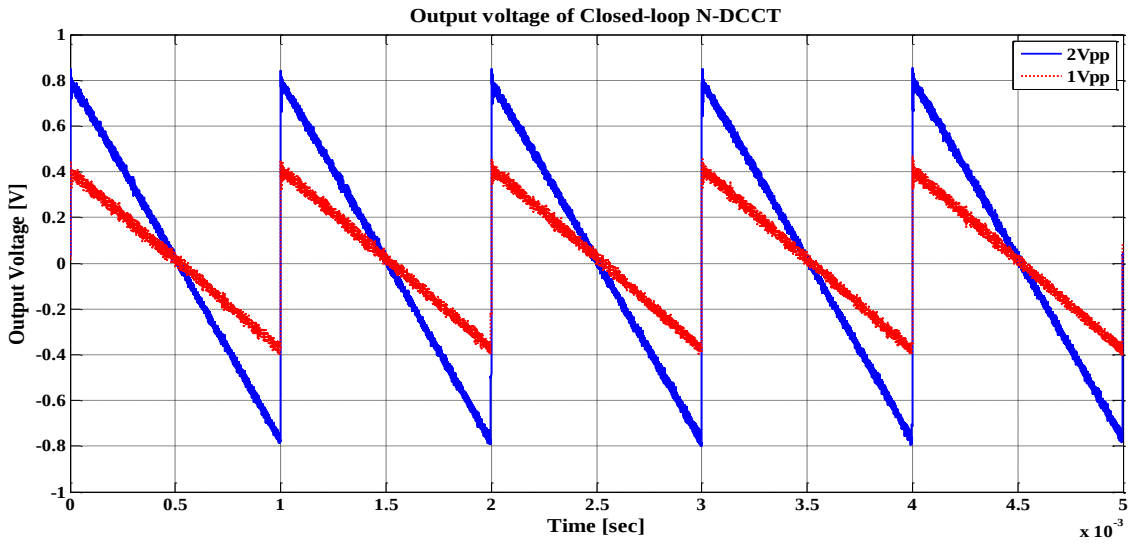

Figure 34 Closed-loop N-DCCT Output Voltage with Ramp Input Signal (Four OPA860)

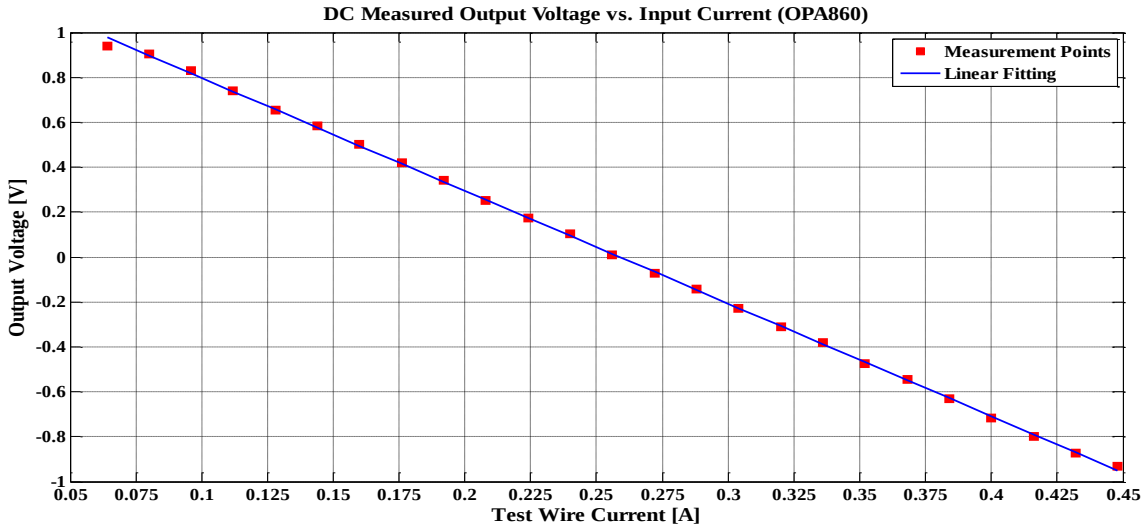

Figure 35 Output Voltage Measurement Result (OPA860) with DC input voltage

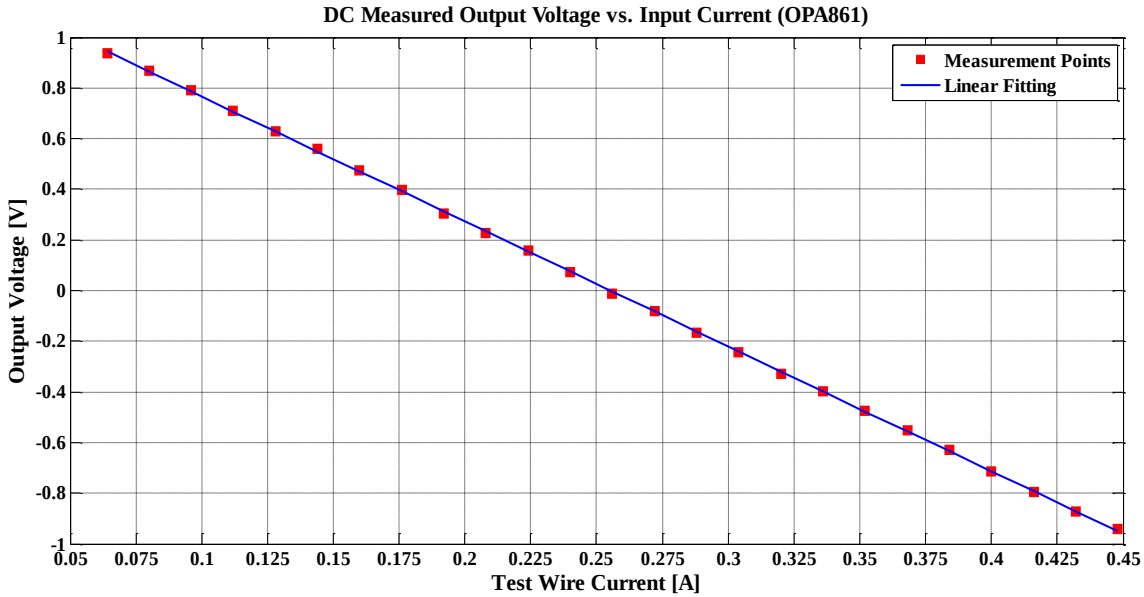

Figure 36 Output Voltage Measurement Result (OPA861) with DC input voltage

Table 7 summarizes the measurement results for the closed-loop N-DCCT. The MR sensor used for this test is TMR45F model. The theoretical sensitivity is calculated at a given nominal value for the feedback system components. However, deviation from this value can be caused by change of the design parameters. For example the "G_{mo}" is given in the datasheet as a range between 80-110mA/V and the theoretical value is calculated at 95mA/V (this is also valid for the parasitic values).

Table 7 Measured Specs of the MR based Closed-loop N-DCCT

OTA Type	Theoritical N-DCCT Sensitivity [V/A]	Measured N-DCCT Sensitivity [V/A]	Output Noise at low frequency [µV/√Hz]	Detectivity [nT/√Hz]	Minimum Detectable Current at DC [µA/√Hz]
OPA860	-7.4852 (Single OTA) to -11.2985 (Four OTA)	-5.02	74.7	1.86	14.88
OPA861		-4.93	40	1.014	8.11

❖ Future Work

After the success of implementing a closed-loop N-DCCT device using discrete electronics components, the following research ideas could be investigated:

1. Real-time testing of the device at GSI and comparing its performance with commercial ones
2. Improving the device sensitivity
3. Improving the device dynamic range
4. Design the system in one ASIC.
5. Design of a digital feedback loop for higher dynamic range and higher resolution

The project team has applied for a new project fund to investigate these proposed ideas. The project proposal was submitted on April 2015 for the "German-Egyptian Research Fund Grant". The proposal was submitted in partnership with "The German University in Cairo". The proposal is still under evaluation.

❖ References

1. W. F. Egelhoff Jr, P. W. T. Pong, J. Unguris, R. D. McMichael, E. R. Nowak, A. S. Edelstein, et al., "Critical challenges for picoTesla magnetic-tunnel-junction sensors," Sensors and Actuators A: Physical, vol. 155, pp. 217-225, 2009.
2. V. Nazarov, H. S. Cho, J. Nowak, S. Stokes, and N. Tabat, "Tunable ferromagnetic resonance peak in tunneling magnetoresistive sensor structures," Applied Physics Letters, vol. 81, pp. 4559-4561, 2002.
3. W. M. Leach, Jr., "Fundamentals of low-noise analog circuit design," *Proceedings of the IEEE*, vol. 82, pp. 1515-1538, 1994.